World Electric Vehicle Journal

MDPI

Article

Application of Improved Ant Colony Algorithm in Optimizing the Charging Path of Electric Vehicles

Zhiqun Qi

School of Computer and Information Engineering, Jiangxi Normal University, Nanchang 330022, China; 002065@jxnu.edu.cn

Abstract: In current traffic congestion scenarios, electric vehicles (EVs) have the problem of reduced battery life and continuous decline in endurance. Therefore, this study proposes an optimization method for electric vehicle charging scheduling based onthe ant colony optimization algorithm with adaptive dynamic search (ADS-ACO), and conducts experimental verification on it. The experiment revealed that in the four benchmark functions, the research algorithm has the fastest convergence speed and can achieve convergence in most of them. In the validation of effectiveness, the optimal solution for vehicle time consumption under the ADS-ACO algorithm in the output of the algorithm with a stationary period and a remaining battery energy of 15 kW·h was 2.146 h in the regular road network. In the initial results of 15 kW·h under changes in road conditions from peak to peak periods, the total energy consumption of vehicles under the research algorithm was 4.678 kW·h and 4.656 kW·h under regular and irregular road networks, respectively. The change results were 4.509 kW·h and 4.656 kW·h, respectively. The initial results of 10 kW·h were 4.755 kW·h and 4.873 kW·h, respectively. The change results were 4.461 kW·h and 4.656 kW·h, respectively, which are lower than the comparison algorithm. In stability verification, research algorithms can find the optimal path under any conditions. The algorithm proposed in the study has been demonstrated to be highly effective and stable in electric vehicle charging path planning. It represents a novel solution for electric vehicle charging management and is expected to significantly enhance the range of electric vehicles in practical applications.

Keywords: electric vehicles; charging path; ADS-ACO; time slice

Citation: Qi, Z. Application of Improved Ant Colony Algorithm in Optimizing the Charging Path of Electric Vehicles. *World Electr. Veh. J.* **2024**, *15*, 230. https://doi.org/10.3390/wevj15060230

Academic Editor: Joeri Van Mierlo

Received: 8 April 2024
Revised: 13 May 2024
Accepted: 20 May 2024
Published: 24 May 2024

1. Introduction

Electric vehicles (EVs) and batteries are the main power sources with clean and pollution-free characteristics, and are considered a promising method to alleviate the current fossil energy problem [1]. EVs, represented by new energy vehicles, are gradually replacing traditional fossil fuel vehicles and becoming a national development consensus and a planning system goal. Due to poor battery life and insufficient construction of charging facilities, current EVs have significantly reduced their competitiveness and lost some market share. Therefore, improving their endurance is the focus of current research [2]. However, most of the current research only analyzes their battery conversion efficiency and charging pile construction layout, with little research on the charging selection behavior and scheduling of traditional EV users [3]. Moreover, some of these studies overlook various constraints and limitations in their actual travel process. In addition, ant colony optimization (ACO) is often used in path optimization because it utilizes the positive feedback mechanism of remaining pheromones on the path between ants for information transmission [4,5]. However, there are still shortcomings in optimizing the charging path of EVs. On the ground of this, this study proposes an optimization method for EV charging scheduling based on the ant colony optimization algorithm with adaptive dynamic search (ADS-ACO). Its purpose is to effectively improve the battery life of EVs and provide a reference value for the path optimization problem of charging scheduling

for users of EVs. In comparison to existing methodologies, this approach enables the dynamic adaptation of the search strategy in accordance with the prevailing circumstances through the incorporation of an adaptive mechanism, thereby facilitating a more effective adaptation to complex environments. The research proposes an innovative approach to path planning, utilizing the ADS-ACO algorithm. This algorithm is capable of achieving more accurate results in dynamic and changing road environments, while also considering various constraints, making it more realistic. The significance of the research lies in its application of the ADS-ACO algorithm to optimize the path of EVs. This approach offers users a superior experience and contributes to the continued evolution of EVs.

The research is divided into four parts. The first part summarizes and discusses the current research on optimizing the charging path of EVs. The second part describes the ACO algorithm and proposes the ADS-ACO algorithm to construct a scheduling model. The third part verifies the effectiveness and stability of the algorithm. The fourth part is a summary of the entire article.

2. Related Work

The current limited battery charge storage capacity of EVs makes the distance between charges increasingly short, and frequent charging is also required, which takes much longer than the conventional fuel refilling process [6]. So not only should we consider the current distribution of charging infrastructure, but also the range that the remaining battery capacity of an EV can travel, which are very challenging scheduling problems [7]. At present, some scholars have conducted research on optimizing the charging path of EVs. Xiang et al. proposed an optimization method for EV charging paths based on event-driven pricing, taking into account the interaction between vehicles in path planning and charging navigation in response to current issues related to EV path planning and charging navigation. This effectively improved the actual range of EVs [8]. Hu et al. addressed the related issues caused by the current lagging charging infrastructure for the popularization of EVs and constructed a corresponding model by proposing charging behavior data in the trajectory of electric taxis. This effectively enhanced the popularity of EVs while improving user satisfaction [9]. Niccolai et al. proposed an optimization method for the layout of charging stations in the development of EVsbased on evolutionary algorithms, which not only improves the service quality of charging stations but also enhances the actual range of EVs [10]. Rajamorthy et al. proposed an optimized scheduling algorithm for EV charging based on the Grey Sail Fish School to address the related issues brought by EVs in the development of intelligent transportation systems. This effectively promoted the development of intelligent transportation systems while improving the endurance of EVs [11].

In addition, Król and Sierpiński proposed a new genetic algorithm for optimizing the location of EV charging equipment in urban road networks based on fuzzy objective functions to address the related issues faced by the development of EVs. This algorithm provided assistance for the development of EVs and thus enhanced user satisfaction [12]. Cui et al. proposed a two-layer optimization model for optimizing the charging path and optimal charging pricing of public EVs in the urban transportation system. This model considers the coupled operation of transportation and power systems. This model not only promotes the development of EV but also reduces some of the burden on users [13]. Li et al. proposed a data-driven planning method for EV charging infrastructure based on market mechanisms to address relevant issues in current EV charging planning. This method not only optimizes the configuration of EV charging, but also promotes the development of EVs [14]. Fakhrmoosavi et al. proposed an optimization method for the layout of EV chargers based on the current issues related to EV charging scheduling, taking into account traffic needs. This method enhanced the endurance of EVs while reducing their time cost [15]. The advantages and disadvantage of each scholar's work are shown in Table 1.

Table 1. Advantages and disadvantages of existing methods.

Method	Lead Author	Advantage	Disadvantage
Event-driven pricing based optimization method for electric vehicle charging path	Xiang et al. [8]	Improved the actual range of electric vehicles	Complex event-driven pricing system required
Charging behavior data model	Hu et al. [9]	Improved the popularity and user satisfaction of electric vehicles	There are situations where data is inaccurate or incomplete
Optimization method for charging station layout based on evolutionary algorithm	Niccolai et al. [10]	Improved the service quality of charging stations and the endurance of electric vehicles	Requires a large amount of computing resources
Optimization scheduling algorithm for electric vehicle charging based on the Grey Sailfish School	Rajamorthy et al. [11]	Improved the endurance of electric vehicles	Complexity and uncertainty
A new genetic algorithm based on fuzzy objective function	Król and Sierpiński [12]	Improved user satisfaction	High computational cost
A double-layer optimization model for charging path optimization and charging pricing optimization	Cui et al. [13]	Promoted the development of electric vehicles and reduced the burden on users	Need to coordinate optimization objectives at different levels
A data-driven electric vehicle charging infrastructure planning method based on market mechanisms	Li et al. [14]	Promoted the development of electric vehicles	Effective market mechanisms and data support are needed
Optimization method for layout of electric vehicle charging stations based on traffic demand	Fakhrmoosavi et al. [15]	Improved the endurance of electric vehicles and reduced time costs	Affected by actual traffic demand and road conditions

Research by domestic and foreign scholars indicates that current research on the charging scheduling problem of EVs has ignored various constraints and limitations in their actual travel process, only considering the static road network environment. Meanwhile, when studying the constant state of roads, it focuses on analyzing changes in road length, but neglects the impact of time-varying speeds and other factors. Therefore, this study comprehensively considers battery energy consumption, traffic conditions, and the distribution of charging stations. Based on the ADS-ACO algorithm, an innovative model for optimizing the charging scheduling path of EVs is constructed.

3. Optimization Analysis of Electric Vehicle Charging Path Based on Improved Ant Colony Algorithm

Compared to other swarm intelligence algorithms, the ACO algorithm has a higher ability to find the optimal solution. Therefore, this section mainly describes the traditional ACO algorithm and improves it based on the actual situation.

3.1. Analysis of Ant Colony Algorithm Based on Adaptive Dynamic Search

This study proposes an optimization method for EV charging scheduling based on the ADS-ACO algorithm to address the issue of reduced battery life and continuous decline in endurance of EVs in current traffic congestion scenarios. The traditional ACO algorithm primarily employs the positive feedback mechanism of the residual pheromones along the path between ants for information transmission, thereby exhibiting robust resilience and the capacity to identify superior solutions [16–18]. The process is shown in Figure 1.

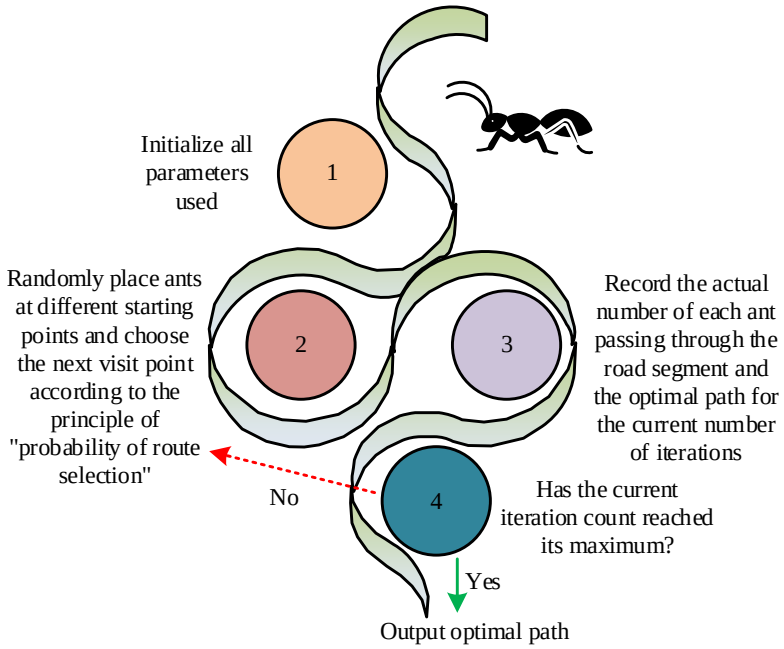

Figure 1. Schematic diagram of the ACO algorithm process.

In Figure 1, the ACO algorithm process first initializes all the parameters used. Secondly, ants are randomly placed at different starting points, and the next visit point is selected according to the principle of "path selection probability", while updating the prohibited list. Next, it records the number of ants passing through the road section and updates the pheromone concentration of each ant passing through the road section in real-time. Finally, it is determined whether the current iteration count has reached the maximum. If not, the ant is placed again to repeat the process, and if so, the optimal path is output. The path selection probability expression of the AOC algorithm is shown in Equations (1) and (2).

$$\psi(j,k) = \frac{1}{c(j,k)} \tag{1}$$

Here, $\psi(j,k)$ represents heuristic information. $c(j,k)$ represents the distance between city points j and k.

$$\gamma^l(j,k) = \begin{cases} \frac{[\mu(j,k)]^\beta * [\psi(j,k)]^\alpha}{\sum_{k \notin tabu_l} [\mu(j,k)]^\beta * [\psi(j,k)]^\alpha}, if\ k \notin tabu_l \\ 0, others \end{cases} \tag{2}$$

Here, $\gamma^l(j,k)$ represents the path selection probability of ant l from city point j to k. $\mu(j,k)$ represents the concentration of pheromones on edge (j,k). $tabu_l$ represents the node where the storage ant l passes through. β represents the heuristic factor. α represents the expected factor. In addition, the traditional expression of pheromone concentration updates is shown in Equations (3) to (5).

$$\mu_{jk}(\tau+1) = (1-\varphi) * \mu_{jk}(\tau) + \Delta\mu_{jk} \tag{3}$$

Here, τ represents the time point. φ represents the volatilization factor of pheromones.

$$\Delta\mu_{jk} = \sum_1^n \Delta\mu_{jk}^l \tag{4}$$

Here, n represents the number of ant colonies.

$$\Delta\mu_{jk}^{l} = \begin{cases} \frac{P}{M_{l,jk}} jk \in m_l \\ 0, others \end{cases} \tag{5}$$

Here, P represents the intensity of pheromones. $M_{l,jk}$ represents the set of road sections passed by the lth ant. ACO algorithms inevitably have problems such as slow convergence. Therefore, research has been conducted to adjust the initial pheromone distribution conditions and the selection transition probability rules for the next node, and introduce genetic mutation operations in genetic algorithms to obtain the current optimal solution. In practical applications, this study needs to consider the traffic flow and road conditions under time-varying speeds and time slots, so different congestion conditions lead to varying probabilities of selecting road sections over time. On the ground of this, the transfer probability expression under the ADS-AOC algorithm is shown in Equation (6).

$$\gamma_{j,k}^{l}(t) = \begin{cases} \frac{\left[\mu_{j,k}(t)\right]^{\beta} * \left[\psi_{j,k}(t)\right]^{\alpha}}{\sum_{k \notin tabu_l} \left[\mu_{j,k}(t)\right]^{\beta} * \left[\psi_{j,k}(t)\right]^{\alpha}} * \rho_{jk}, if\ k \notin tabu_l \\ 0, others \end{cases} \tag{6}$$

Here, ρ_{jk} represents the road congestion coefficient between j and k [19]. To enable the ant colony to find the optimal path at the beginning of the iteration, this study proposes a new initial pheromone allocation method. The relevant expression is shown in Equation (7).

$$\mu_{j,k}(0) = \begin{cases} \mu_0 + \frac{P}{M_{jk}}, \text{The path passed by the greedy algorithm} M_{j,k} \\ \mu_0, others \end{cases} \tag{7}$$

Here, μ_0 represents the initialization pheromone of each road segment. The volatility factor is an important factor that affects the global search ability and convergence speed of ant colony algorithms. It is usually set to a fixed value. In this study, to avoid slow convergence or falling into local optima, the volatility factor is set to a large value in the early stages of the algorithm, and after reaching a certain number of iterations, the pheromone volatility coefficient is gradually reduced. The relevant expressions are shown in Equation (8).

$$\varsigma = \begin{cases} 0.7, 0 < H_b \leq \frac{H_{\max}}{3} \\ 0.4\left(2 - \frac{H_b}{H_{\max}}\right), \frac{H_{\max}}{3} < H_b \leq \frac{2H_{\max}}{3} \\ 0.4, \frac{2H_{\max}}{3} < H_b \leq H_{\max} \end{cases} \tag{8}$$

Here, ς represents the volatilization factor. H represents the number of iterations [20].

3.2. Construction of Electric Vehicle Charging Scheduling Model Based on Improved Ant Colony Algorithm

Based on the ADS-ACO algorithm, this study aims to optimize the user's remaining battery power from the point of occurrence to the charging station while minimizing road travel time, and constructs a relevant scheduling model based on this. Among these aims, the remaining electricity prediction is usually estimated using the Coulomb counting method. Then, all available battery capacity can be expressed as shown in Equation (9).

$$E_v = E_{\max} - E_e \tag{9}$$

Here, E_v represents all available battery capacity. $E_{\max}$ represents the battery capacity in a fully charged state. E_e represents the utilized battery capacity. The expression of the remaining battery capacity is shown in Equation (10).

$$F_v = F_{\max} - \frac{E_v}{E_{\max}} \tag{10}$$

Here, F_v represents the remaining battery level. $F_{\max}$ represents the battery level when the battery is fully charged. According to relevant regulations, the road congestion coefficient sets the degree of traffic congestion on the main line to four levels: severe congestion, moderate congestion, mild congestion, and unobstructed traffic. Therefore, the calculation expression of ρ in Equation (6) is shown in Equation (11).

$$\rho \begin{cases} 1, v \in [45, 80), \text{Smooth road sections} \\ 0.75, v \in [30, 45), \text{Mild congestion on the road section} \\ 0.5, v \in [20, 30), \text{Moderate congestion on the road section} \\ 0.25, v \in [0, 20), \text{Severe congestion on the road section} \end{cases} \tag{11}$$

Here, v represents the average speed of EVs on this road section. The unit mileage electricity consumption of urban main roads is expressed in Equation (12).

$$\Delta F = 0.004v - 0.179 + \frac{5.492}{v} \tag{12}$$

Here, ΔF represents the unit mileage electricity consumption of urban main roads. The expression of battery energy consumption when an EV passes a certain road section is shown in Equation (13).

$$F_r = \Delta F \times M_r \tag{13}$$

Here, M_r represents the length of section r. Due to the relatively simple physical structure of the transportation network analyzed in the study, only the common topological relationships of separation, adjacency, and intersection are used, and the original method is used to construct a road network topology structure diagram. This divides the main road routes of the city into horizontal and vertical routes, and the road network model constructed based on this is shown in Figure 2.

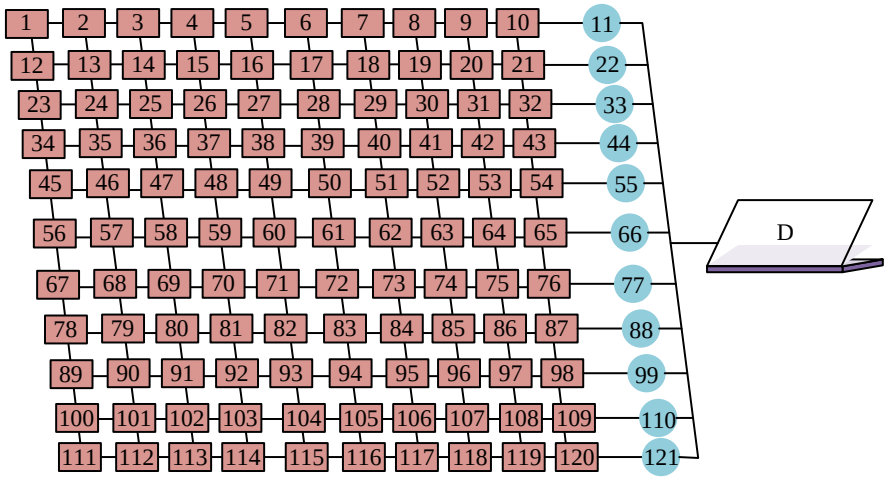

Figure 2. Schematic diagram of road network model.

Figure 2 shows that the study considers the intersection of two road sections as corresponding nodes. Assuming that the number of horizontal and vertical road sections is 10, it indicates that there are 11 charging stations on the main road where EVs arrive at their destination. EVs can form a completed 1D path from starting point 1 to ending point D. The optimization goal of this study is to ensure that when users arrive at the charging station from their departure point, the remaining battery power of the user can reach the shortest time required for the entire road section of the charging station. On the ground of this, the objective function expression of the research model is shown in Equation (14).

$$\begin{cases} \min R_x = R_h + R_y + R_q + R_z \\ F_i > F_x \end{cases} \tag{14}$$

Here, R_x represents the total driving time. R_h represents the time taken by the user from the starting point to the charging station. R_y represents the time the user waits for traffic lights and charging queues on the road. R_q represents the charging time of EV. R_z represents the time when the user arrives at their destination from the charging station. F_i represents the remaining battery energy consumption of the EV at the starting point. F_x represents the total energy consumption from the starting point to the charging station. The expression of model constraints is shown in Equation (15).

$$\begin{cases} F_{fn}^{X} = M_{i,fn} \times \Delta F; F_{mn}^{Y} = M_{v,mn} \times \Delta F; F_h = \sum_f \sum_n F_{fn}^{X} + \sum_n \sum_m F_{nm}^{Y} \\ F_x = F_h + F_g; R_h = \sum_f \sum_n \dfrac{M_{i,fn}}{v} + \sum_m \sum_n \dfrac{M_{v,mn}}{v}, F_d = F_i - F_x \\ R_q = \dfrac{90\%F_{\max} - F_d}{\lambda\omega}, v_{jk} = V * \rho \end{cases} \tag{15}$$

Here, X and Y represent horizontal and vertical sections, respectively. $M_{i,fn}$ represents the length of section X_{fn}. $M_{v,mn}$ represents the length of section Y_{mn}. F_h represents the total energy consumption of horizontal and vertical roads. F_x represents the total energy consumption of the user from the starting point to the charging station. F_g represents the sum of other energy consumption of the EV besides driving energy consumption. F_d represents the remaining battery energy consumption from the user's starting point to the charging station. λ represents fast charging power. ω represents the fast charging efficiency. V represents the speed of the EV at the starting point. Based on the objective optimization model, this study uses the ADS-ACO algorithm to solve it, and classifies the traffic flow into stable and changing road conditions based on different time slots. The solution diagram of the ADS-ACO algorithm scheduling model with a starting point set under time-varying speed and stable road conditions is shown in Figure 3.

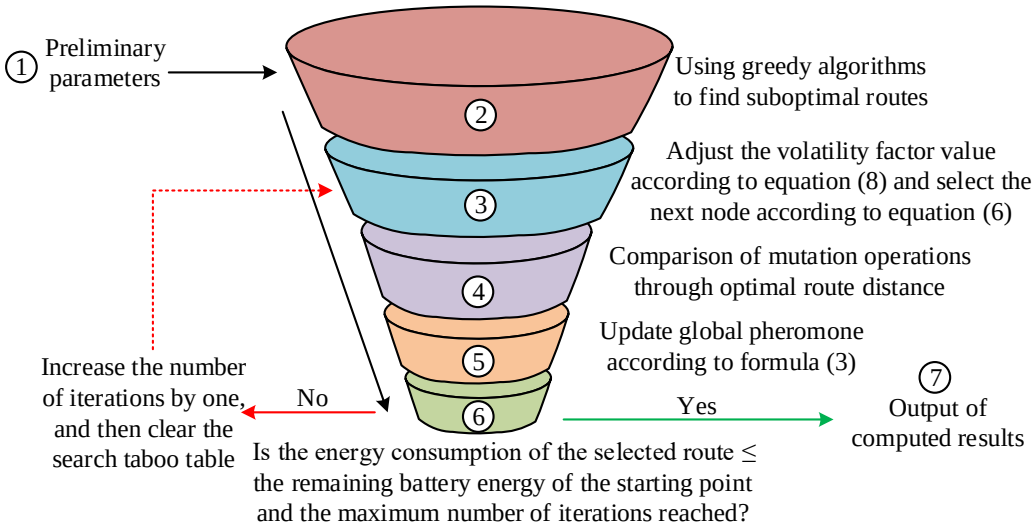

Figure 3. Schematic diagram of ADS-ACO algorithm scheduling model for setting starting points in time slices with time-varying speeds and stable road conditions.

In Figure 3, the black arrow represents the execution steps of the algorithm from 1 to 6, the red solid line arrow represents the flow direction that does not meet the judgment rule, the red dashed line arrow represents the flow direction that returns to step 3, and the green arrow represents the flow direction that meets the judgment rule. Figure 3 shows that when the starting point is fixed, the algorithm first initializes the parameters and uses the greedy algorithm to find the suboptimal route. Secondly, it adjusts the volatility factor value according to Equation (8) and selects the next node according to Equation (6), and adds it to the taboo table. Then, the optimal route distance is used for mutation operation comparison to screen out the optimal route and obtain the optimal path. Then, according to Equation

(3), the global pheromone is updated and the selected optimal solution is determined. If the battery energy consumption of the selected route is less than or equal to the remaining battery energy at the starting point of the EV and the maximum number of iterations is reached, the result is output. Otherwise, the volatilization factor is dynamically adjusted to repeat the process. The remaining changes in road conditions or random starting points will not be described too much here.In the performance analysis of the model, four benchmark functions are introduced: Rosenbrook function, Schwefel function (Schwefel 2.2), Griewank function, and Rastigin function. The formula is shown in Equation (16).

$$\begin{cases} f(x) = \sum_{i=1}^{n-1}\left[100 \times (x_{i+1} - x_i^2)^2 + (x_i - 1)^2\right] \\ f'(x) = \sum_{i=1}^{n} |x_i| + \prod_{i=1}^{n} \cos(\frac{x_i}{\sqrt{i}}) \\ f''(x) = 1 + \frac{1}{4000}\sum_{i=1}^{n} x_i^2 - \prod_{i=1}^{n} \cos(\frac{x_i}{\sqrt{i}}) \\ f'''(x) = 10n + \sum_{i=1}^{n}\left[x_i^2 - 10\cos(2\pi x_i)\right] \end{cases} \tag{16}$$

Here, $f(x)$ represents the Rosenbrook function, $f'(x)$ represents the Schwefel 2.2 function, $f''(x)$ represents the Griewank function, $f'''(x)$ represents the Rastigin function, and $x = (x_1, x_2, \ldots, x_n)$ represents a n-dimensional vector. The Rosenbrock function is employed to assess the efficacy of algorithms in navigating complex search spaces. The Schwefel 2.22 function is utilized to gauge an algorithm's capacity to adapt to highly nonlinear problems with a multitude of local minima and steep slopes. The Griewank function is utilized to evaluate an algorithm's effectiveness in addressing multimodal optimization problems. The Rastigin function is employed to assess an algorithm's global search capability when confronted with highly multimodal and nonlinear problems.

3.3. Constraints

The limitations imposed on horizontal and vertical road segments can mirror the topographical configuration of the road network. This constraint ensures that the driving route from the starting point to the charging station is viable. In the event that this constraint cannot be met, the algorithm will be unable to identify a feasible path solution, thereby preventing the acquisition of effective optimization results. The constraint on total energy consumption ensures that the actual energy consumption of EVs from the starting point to the charging station does not exceed the upper limit of the remaining electricity at the starting point. Should this constraint be breached, even if the algorithm identifies the shortest path in a timely manner, it may not be possible to achieve it due to insufficient battery power, thereby affecting the feasibility and effectiveness of the algorithm. The constraint on the remaining power of EVs ensures that they will still have sufficient remaining power upon arrival at the charging station, thereby meeting the goal of minimizing travel time. In the event that the remaining battery capacity upon departure is insufficient, the algorithm may be unable to identify a viable path plan, which has a detrimental impact on the optimization outcome. The capacity to rapidly recharge is indicative of the performance of the charging station and directly correlates with the charging time of EVs at the charging station, thereby influencing the efficacy of the total travel time objective. A low level of charging power and efficiency will result in a lengthy charging time, which in turn constrains the potential for optimization in the total driving time. The initial motion state constraint of an EV reflects its driving characteristics, which can influence the travel time from the starting point to the charging station. A reduction in the initial speed will result in an increase in travel time, which in turn will affect the optimization effect of the algorithm on the total travel time.

4. Simulation Analysis of Algorithm Performance and Scheduling Model Performance

To verify the effectiveness of the proposed optimization model for EV charging paths, this study introduced the traditional ACO algorithm and the ant colony system with pseudorandom state transition rules (ACS-PSTR) as a comparative method to conduct experiments on four different benchmark test functions. The four benchmark functions are Rosenbrook function, Schwefel function (Schwefel 2.2), Griewank function, and Rastigin function. In addition, this experiment set the number of ant colonies, iteration times, and benchmark test functions to 300, 200, and 10 dimensions, respectively. Accordingly, the results of the Rosenbrock and Schwefel 2.2 functions are shown in Figure 4.

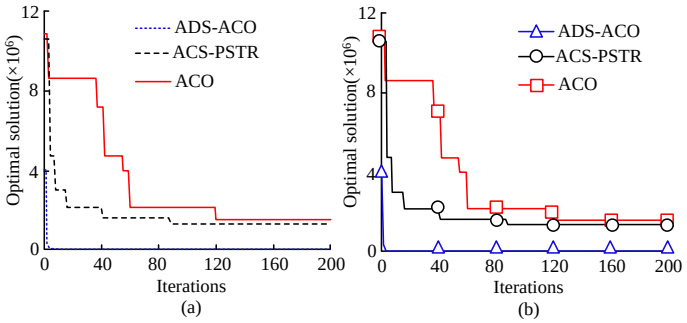

Figure 4. Test results of different methods on Rosenbrock and Schwefel 2.2 functions: (**a**) Comparison in Rosenbrock; (**b**) Comparison in Schwefel 2.2.

To verify the effectiveness of the proposed EV charging path optimization model, the study first set the number of ant colonies, iteration times, and benchmark test functions to 300 and 200, respectively. The specific parameter settings are shown in Table 2.

Table 2. Experimental parameter settings.

Parameter	Parameter Values
Heuristic factor	1
Desirable factors	5
Volatilization factor	5
Ant colony size	300
Pheromone concentration constant	100
Iterations	200

Then, the study introduced the traditional ACO algorithm and the ACS-PSTR as comparison methods, and conducted experiments on four different benchmark test functions with a benchmark function dimension of 10. The four benchmark functions are Rosenbrook function, Schwefel function (Schwefel 2.2), Griewank function, and Rastigin function. Accordingly, the results of the Rosenbrock and Schweefel 2.2 functions are shown in Figure 4.

Figure 4 comprehensively shows that in the Rosenbrock function, the ADS-ACO algorithm converges when the number of iterations is around four, and the optimal solution gradually approaches zero.In the Schwefel 2.2 function, the ADS-ACO algorithm converges when the optimal solution reaches zero with approximately three iterations. The results of the Griewank function and Rastigin function are shown in Figure 5.

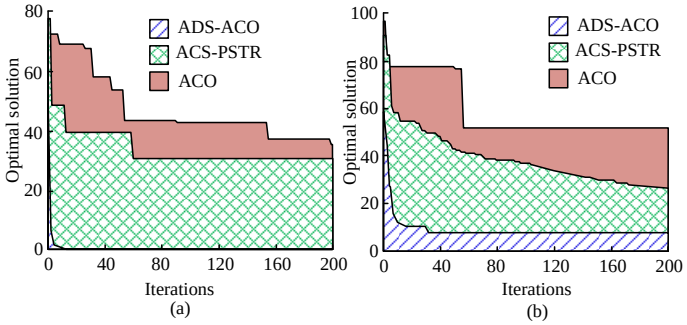

Figure 5. Results on Griewank function and Rastigin function: (**a**) Comparison in Griewank; (**b**) Comparison in Rastigin.

Figure 5 comprehensively shows that the ADS-ACO algorithm in the Griewank function achieves convergence when the number of iterations is around 10.The ADS-ACO algorithm performs equally well in the Rastigin function. Overall, the ADS-ACO algorithm performs best in the four basic functions. On this basis, the study takes a total of 16 roads in a certain city in the east as the analysis object, with 16 roads set at 1–16. The specific data and distribution of the number of charging stations are shown in Table 3.

Table 3. Geographical location and building density of 16 streets.

Road Number	A	B	C	D	E	Charging Station Number	Node Number	Number of Charging Stations
1	1	2	2.8	9.3	S	a	11	2
2	2	3	1.1	10.1	S	b	22	28
3	3	4	1.9	8.4	S	c	33	2
4	4	5	2.3	10.6	S	d	44	8
5	5	6	2.1	14.1	S	e	55	2
6	6	7	2.8	13.5	S	f	66	12
7	1	12	2.7	11.7	S	g	77	22
8	12	23	2.4	8.2	S	h	88	16
9	23	34	2.6	11.0	K	i	99	5
10	34	45	2.0	11.2	K	j	110	8
11	45	56	2.7	25.7	M	k	121	2
12	56	67	1.3	16.4	K	l	132	2
13	67	78	2.0	11.5	K	m	145	10
14	78	89	2.4	19.4	K	n	154	17
15	89	100	2.3	18.4	K	o	165	4
16	100	111	1.5	16.8	K	/	/	/

In Table 3, A~E represent the starting and ending nodes, total route length (km), real-time traffic flow speed (km/h), and traffic status, while K and M represent severe and moderate congestion. Table 1 shows that the 16 road starting nodes are named by the serial numbers in Figure 2, and are numbered 1–16 from node 1 to node 111. Among them, the maximum total length of the route is 2.8 km.The maximum real-time traffic speed is 25.7 km/h. Therefore, in the case of extreme effectiveness of the ADS-ACO algorithm, the actual road conditions include stable and changing road conditions. Simulation tests are conducted on regular (G) and irregular road networks (N) with a remaining battery power of 15 kW·h and 10 kW·h, respectively. Meanwhile, its initial speed is set to 50 km/h, the maximum number of iterations is 150, the maximum battery capacity is 120 kW, and the fast charging energy is 120 kW·h. Due to the fact that there are 16 actual roads, this study has expanded the road network model in Figure 2 and compared the greedy algorithm (T), ACO algorithm (J), and research algorithm (Y). Accordingly, the output results of the EV battery remaining energy of 15 kW·h and 10 kW·h under the road network model

with different starting points for stable road conditions during stable and peak periods are shown in Figure 6.

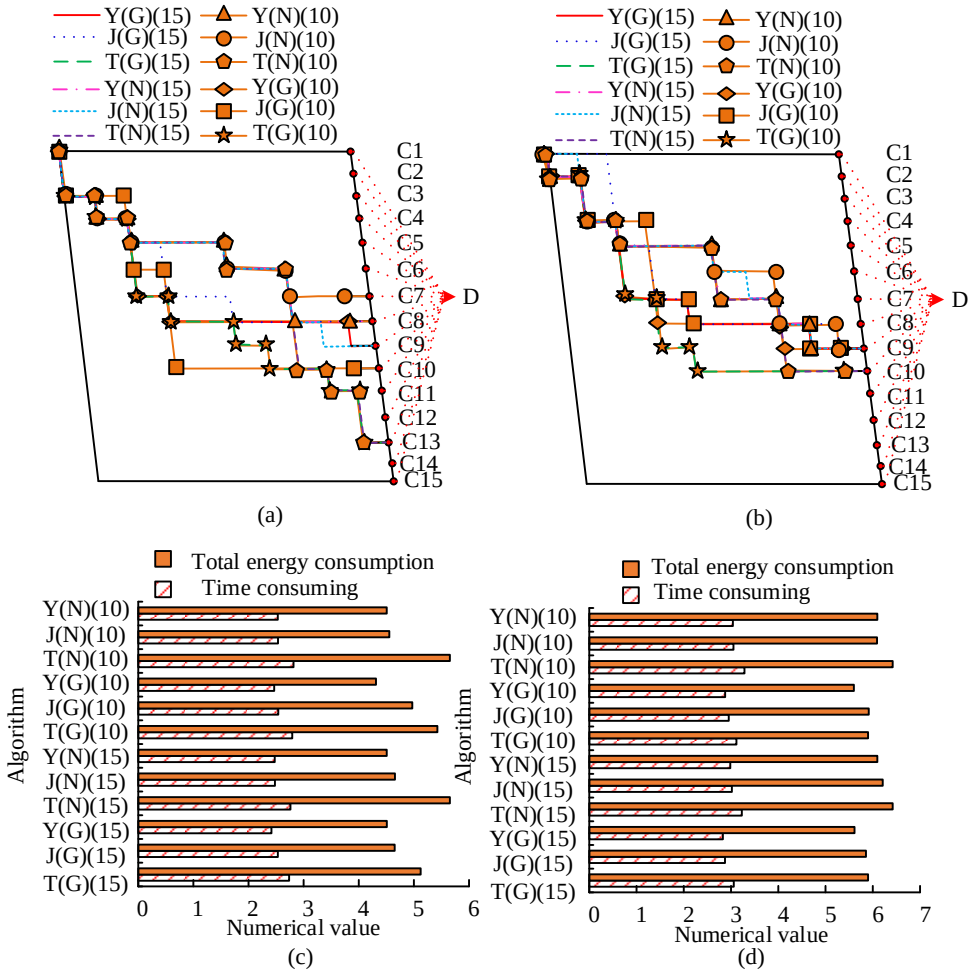

Figure 6. Output results of remaining electrical energy of 15 kW·h and 10 kW·h under stable road conditions during stable and peak periods: (**a**) Set the starting point for stable road conditions during the stable period and follow the driving path; (**b**) Set the starting point for stable road conditions during peak hours and follow the driving path; (**c**) Stable period results; (**d**) Results during summit periods.

In Figure 6, the red arrow mainly indicates the direction and flow of the target node or process. Figure 6 comprehensively shows that the optimal solution for vehicle time consumption under the ADS-ACO algorithm is 2.146 h in a regular road network during the stationary period with a remaining battery energy of 15 kW·h. The total energy consumption of the irregular road network during peak hours is 6.096 kW·h, which is lower than the comparison algorithm. Overall, ADS-ACO has a high effectiveness. Accordingly, the initial result output and change result output of the remaining battery energy of 15 kW·h and 10 kW·h under different road networks with different starting points during peak to flat peak road conditions are shown in Figure 7.

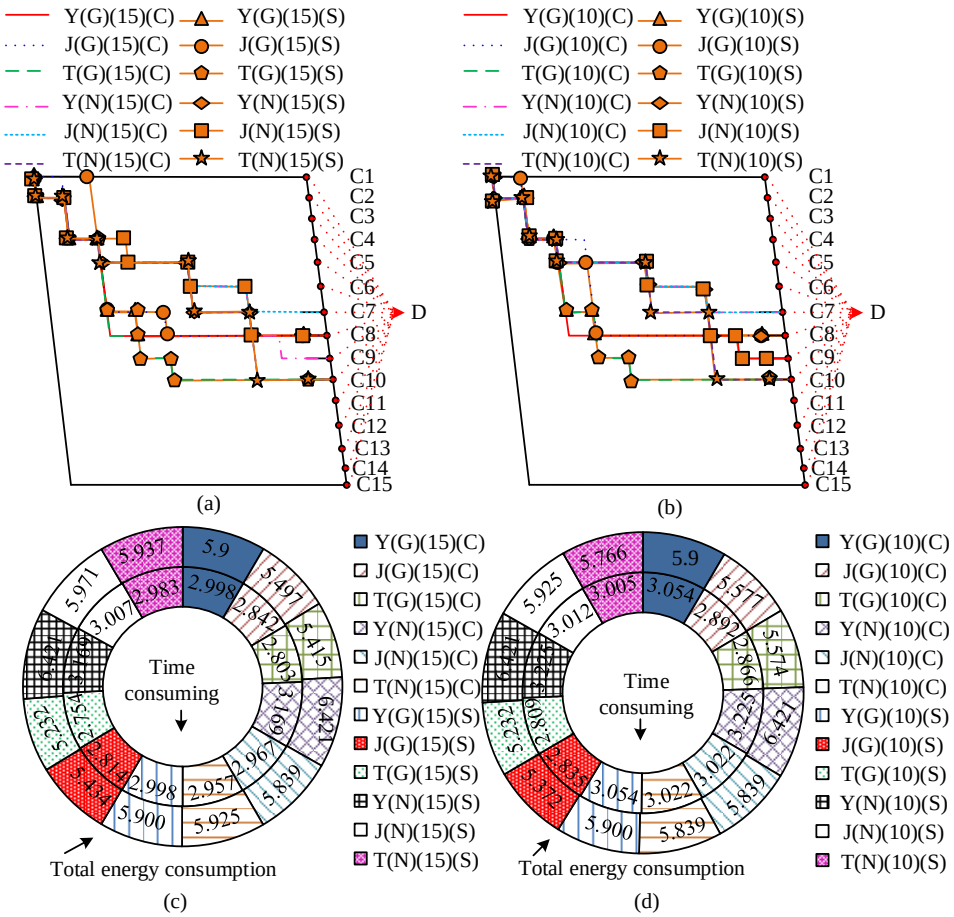

Figure 7. Output of the initial and changing results of the remaining battery energy of 15 kW·h and 10 kW·h under changes in road conditions from peak to flat peak: (**a**) Path of 15 kW·h from peak to flat peak; (**b**) Path of 10 kW· h from peak to flat peak; (**c**) Results of 15 kW·h from peak to flat peak periods; (**d**) Results of 10 kW·h from peak to flat peak periods.

In Figure 7, the red arrow mainly indicates the direction and flow of the target node or process. In Figure 7, C represents the initial result and S represents the changed result, The inner ring represents the optimal solution, while the outer ring represents the total driving energy consumption. Figure 7 shows that the total energy consumption output of the 15 kW·h change in road conditions from peak to peak periods in regular and irregular road networks is 5.232 kW·h and 5.937 kW·h, respectively. The total energy consumption output from the initial results of 10 kW·h is 5.232 kW·h and 5.766 kW·h, respectively, which are lower than the comparison algorithm. In addition, the initial result output and change result output of the remaining battery energy of 15 kW·h and 10 kW·h under different road networks with different starting points under changes in road conditions from peak to peak periods are shown in Figure 8.

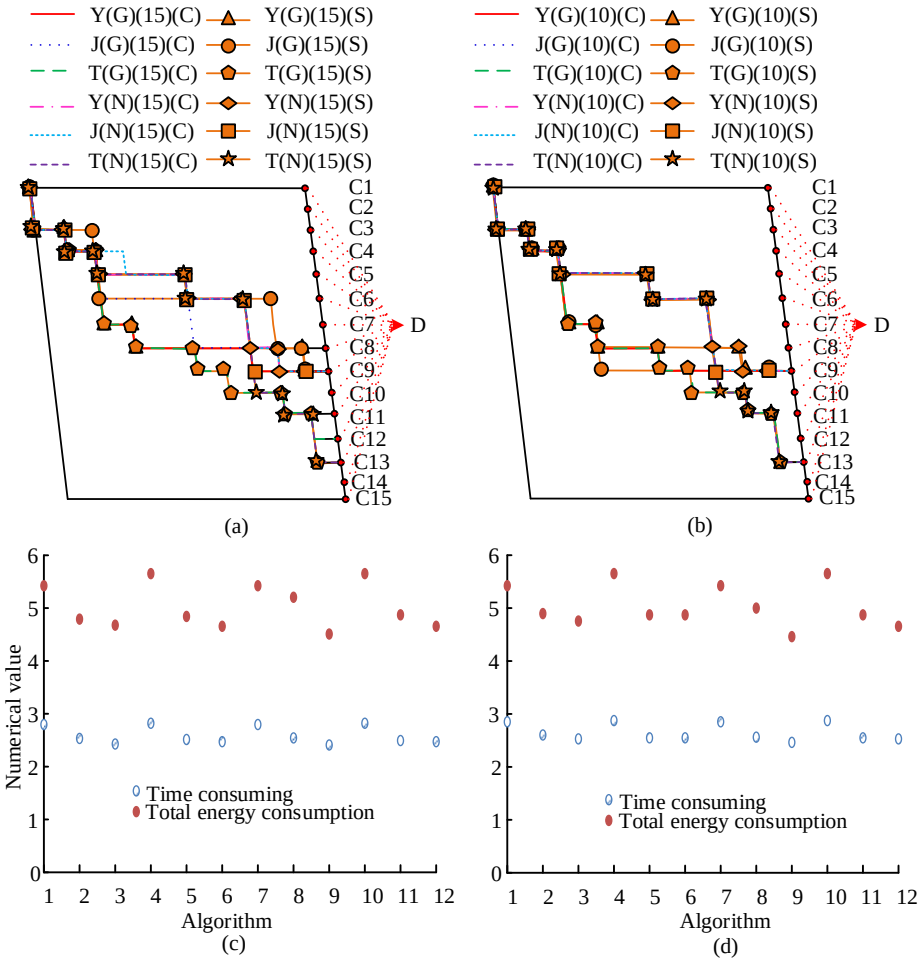

Figure 8. Output of the initial and changing results of the remaining battery energy of 15 kW·h and 10 kW·h under changes in road conditions from peak to peak periods: (**a**) Path from flat peak to peak 15 kW·h; (**b**) Path from flat peak to peak 10 kW·h; (**c**) Results of 15 kW·h from peak to peak periods; (**d**) Results of 10kW·h from peak to peak periods.

In Figure 8, the red arrow mainly indicates the direction and flow of the target node or process. The horizontal axes 1–12 in the figure are consistent with the legends in Figure 7a,b. Figure 8 shows that in the initial result of 15 kW·h, the total energy consumption of the vehicle under the regular road network, is 4.678 kW·h, while in the variation result, it is 4.509 kW·h. The initial result of 10 kW·h is 4.755 kW·h, and the variation result is 4.461 kW·h, both lower than the comparison algorithm. Figures 6–8 demonstrate that the ADS-ACO algorithm is able to dynamically adapt the path based on varying road network models with different speeds and time slices for road condition changes. This results in the lowest travel time and total energy consumption, which demonstrates the algorithm's effectiveness. In the stability verification experiment, users are set to start from different starting points, and due to space limitations, only stable road conditions during stable periods and changes in road conditions from peak to stable periods are analyzed. The results of the remaining EV battery energy of 15 kW·h and 10 kW·h at random starting points under stable road conditions during peak periods are shown in Table 4.

Table 4. The results of stable road conditions at random starting points during normal and peak periods.

-	Route	T (h)	Z (kW·h)
1 (1)	1 → 12 → 23 → 24 → 35 → 36 → 47 → 58 → 69 → 70 → 81 → 82 → 83 → 94 → 95 → 96 → 97 → 98 → C9	2.481	4.755
2 (56)	56 → 67 → 78 → 79 → 80 → 81 → 82 → 83 → 94 → 95 → 96 → 97 → 98 → C9	1.931	2.879
3 (45)	45 → 46 → 47 → 58 → 69 → 70 → 81 → 82 → 83 → 84 → 85 → 86 → 87 → C8	1.948	2.735
4 (78)	78 → 79 → 80 → 81 → 82 → 83 → 84 → 85 → 86 → 87 → C8	1.772	1.987
5 (100)	100 → 101 → 102 → 103 → 104 → 105 → 106 → 107 → 108 → 119 → 120 → C11	1.846	2.605
1 (89)	89 → 100 → 101 → 102 → 103 → 104 → 105 → 106 → 107 → 108 → 109 → C10	1.878	2.686
2 (45)	45 → 46 → 47 → 58 → 69 → 70 → 81 → 82 → 83 → 84 → 85 → 86 → 87 → C8	2.004	2.735
3 (78)	78 → 79 → 80 → 81 → 82 → 83 → 84 → 85 → 86 → 87 → C8	1.828	1.987
4 (111)	111 → 112 → 113 → 114 → 125 → 127 → 128 → 129 → 139 → 124 → 142 → C13	1.990	1.989
5 (12)	12 → 23 → 24 → 35 → 36 → 47 → 58 → 69 → 70 → 81 → 82 → 83 → 94 → 95 → 96 → 97 → 98 → C8	2.390	4.258

In the first column of Table 4, 1–5 represents the starting order, with node names in parentheses. T represents time consumption and Z represents total energy consumption. The first five rows show the results at 15 kW·h, while the last five rows show the results at 10 kW·h. Table 2 shows that among the remaining battery energy of 15 kW·h, the fourth departure node 78 has the lowest total energy consumption, which is 1.987 kW·h. Overall, the charging scheduling planning route of the ADS-ACO algorithm can always obtain a suitable path from a random starting point under a regular road network under stable road conditions. The initial and variation results of EV battery residual energy of 10 kW·h under the random starting point of road condition changes from peak to peak periods are shown in Table 5.

Table 5. Initial and variation results of 10 kW·h under random starting point of road condition changes from peak period to peak period.

-	Route	T (h)	Z (kW·h)
1 (133)	13 → 134 → 135 → 136 → 137 → 138 → 139 → 140 → 151 → 162 → 163 → 164 → C15	2.709	4.461
2 (12)	12 → 13 → 24 → 35 → 36 → 47 → 58 → 69 → 70 → 81 → 92 → 103 → 104 → 105 → 106 → 107 → 108 → 109 → C10	2.679	4.814
3 (67)	67 → 68 → 69 → 70 → 81 → 92 → 103 → 104 → 105 → 106 → 107 → 108 → 109 → C10	2.130	2.785
4 (45)	45 → 56 → 67 → 68 → 69 → 70 → 81 → 82 → 83 → 84 → 85 → 86 → 87 → C8	2.214	2.961
5 (89)	89 → 100 → 101 → 102 → 103 → 104 → 105 → 106 → 107 → 108 → 109 → C10	2.054	2.537
1 (133)	133 → 134 → 135 → 136 → 137 → 148 → 149 → 150 → 151 → 162 → 163 → 164 → C15	3.017	5.802
2 (12)	12 → 13 → 24 → 35 → 36 → 47 → 58 → 69 → 70 → 81 → 92 → 103 → 104 → 105 → 106 → 107 → 108 → 109 → C10	2.679	4.814
3 (67)	67 → 68 → 69 → 70 → 81 → 82 → 83 → 84 → 85 → 96 → 97 → → 98 → C9	2.086	2.637
4 (45)	45 → 56 → 67 → 68 → 69 → 70 → 81 → 82 → 83 → 84 → 85 → 86 → 87 → C8	2.214	2.961
5 (89)	89 → 100 → 101 → 102 → 103 → 104 → 105 → 106 → 107 → 108 → 109 → C10	2.054	2.537

Table 5 shows that the total driving energy consumption in the initial and changed output from peak to peak periods is the lowest at the fifth departure node 89, which is 2.537 kW·h. In summary, the ADS-ACO algorithm dynamically adjusts each starting point based on the current road conditions in response to changing road conditions, thereby reducing energy consumption and time, and resolving the charging scheduling route planning problem that needs to be solved in research. This demonstrates the algorithm's high stability. To ascertain the stability of the three algorithms, this study maintained the total number of vertical road sections constant and altered the total number of horizontal road sections by setting the number of charging stations as a scalar. This allowed for the comparison of the algorithms under varying conditions. The results are shown in Figure 9.

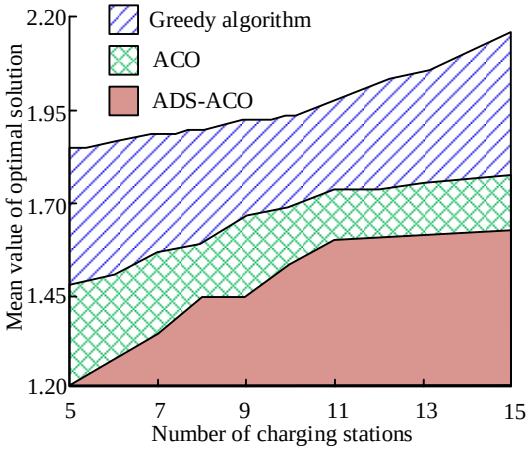

Figure 9. Comparison of stability of three algorithms in the same environment.

Figure 9 shows that as the number of charging stations increases, the total number of horizontal sections also gradually increases, leading to an increase in the global optimal solutions of the three algorithms. However, under the same number of charging stations, the average value of the optimal solution of the ADS-ACO algorithm is always optimal, proving its superior stability. Overall, the ADS-ACO algorithm has high accuracy in EV charging path planning, and it has high effectiveness and stable characteristics, with a wider range of applications. Simultaneously, the algorithm has been demonstrated to be effective in a road network comprising 16 roads with starting nodes ranging from 1 to 111. Furthermore, the algorithm has been shown to be capable of handling large-scale road networks, and to be resilient to changes in network scale and topology. This evidence supports the assertion that the algorithm is scalable. Furthermore, the algorithm is executed on numerous occasions under disparate starting points and conditions, consistently outperforming the comparison algorithm in terms of travel time and energy consumption. Additionally, it maintains optimality in the average optimal solution when the number of horizontal sections increases, thereby corroborating its reliability.

5. Conclusions

This study proposes an optimization method for EV charging scheduling on the ground of the ADS-ACO algorithm to address the issue of reduced battery life and continuous decline in endurance of EVs in current traffic congestion scenarios, and verifies its effectiveness. The experiment demonstrated that in the Rosenbrock function, the ADS-ACO algorithm converges at around four iterations, where the optimal solution gradually approaches zero and performs best in the other three benchmark functions. In the effectiveness verification, the optimal solution for vehicle time consumption under the ADS-ACO algorithm in the output of the stationary period with a remaining battery energy of 15 kW·h was 2.146 h in the regular road network. The total energy consumption of irregular road networks during peak hours was 6.096 kW·h. The total energy consumption output of the 15 kW·h change in road conditions from peak to peak periods in regular and irregular road networks was 5.232 kW·h and 5.937 kW·h, respectively. The total energy consumption output from the initial results of 10 kW·h was 5.232 kW·h and 5.766 kW·h, respectively, which were lower than the comparison algorithm. In the algorithm stability verification, the total energy consumption of the fourth departure node 78 in the EV battery with a residual energy of 15 kW·h at a random starting point during the peak period was 1.987 kW·h. Overall, the ADS-ACO algorithm has high accuracy in EV charging path planning, and has high effectiveness and stability, with a wider range of applications. Nevertheless, when conducting simulation model testing experiments, the number of referenced comparative algorithms is relatively limited, which may not fully evaluate the performance of the ADS-ACO algorithm. Future work will include the implementation of additional swarm intelligence algorithms for horizontal comparison, with the objective of comprehensively

evaluating the advantages and disadvantages of the ADS-ACO algorithm. Additionally, the study did not consider the impact of practical factors such as the layout of charging facilities and fluctuations in electricity prices on the charging behavior of EVs. Future research will expand the model further and consider additional practical factors in order to enhance the practicality and applicability of the algorithm.

Funding: This research received no external funding.

Data Availability Statement: The data presented in this study are available on request from the corresponding author.

Conflicts of Interest: The authors declare no conflict of interest.

Nomenclature

Symbol	Meaning
$\psi(j,k)$	Heuristic information
$c(j,k)$	The distance between city points j and k
$\gamma^l(j,k)$	The path selection probability of ant l from city point j to k
$\mu(j,k)$	The concentration of pheromones on edge (j,k)
$tabu_l$	The node where the storage ant l passes through
β	The heuristic factor
α	The expected factor
τ	The time point
φ	The volatilization factor of pheromones.
n	The number of ant colonies
P	The intensity of pheromones
$M_{l,jk}$	The set of road sections passed by the lth ant
ρ_{jk}	The road congestion coefficient between j and k
μ_0	The initialization pheromone of each road segment
ς	The volatilization factor
H	The number of iterations
E_v	All available battery capacity
$E_{\max}$	The battery capacity in a fully charged state
E_e	The utilized battery capacity
F_v	The remaining battery level
v	The average speed of EV on this road section
ΔF	The unit mileage electricity consumption of urban main roads
M_r	The length of section r
R_x	The total driving time
R_h	The time taken by the user from the starting point to the charging station
R_y	The time the user waits for traffic lights and charging queues on the road
R_q	The charging time of EV
R_z	The time when the user arrives at their destination from the charging station
F_i	The remaining battery energy consumption of the electric vehicle at the starting point
F_x	The total energy consumption from the starting point to the charging station
X	Horizontal section
Y	vertical sections
$M_{i,fn}$	The length of section X_{fn}
$M_{v,mn}$	The length of section Y_{mn}
F_h	The total energy consumption of horizontal and vertical roads
F_x	The total energy consumption spent by the user from the starting point to the charging station
F_g	The sum of other energy consumption of EV besides driving energy consumption

F_d	The remaining battery energy consumption from the user's starting point to the charging station
λ	Fast charging power
ω	The fast charging efficiency
V	The speed of the electric vehicle at the starting point
$f(x)$	The Rosenbrook function
$f'(x)$	The Schwefel 2.2 function
$f''(x)$	The Griewank function
$f'''(x)$	The Rastigin function
$x = (x_1, x_2, \ldots, x_n)$	a n-dimensional vector

References

1. Leite, M.R.C.O.; Bernardino, H.S.; Gonçalves, L.B. A variable neighborhood descent with ant colony optimization to solve a bilevel problem with station location and vehicle routing. *Appl. Intell.* **2022**, *52*, 7070–7090. [CrossRef]
2. Makeen, P.; Memon, S.; Elkasrawy, M.A.; Abdullatif, S.O.; Ghali, H.A. Smart green charging scheme of centralized electric vehicle stations. *Int. J. Green Energy* **2022**, *19*, 490–498. [CrossRef]
3. Wang, M.; Xie, Q. Logistics pure electric vehicle routing based on GA-PSO Algorithm. *Mechanics* **2023**, *29*, 235–242. [CrossRef]
4. Devendiran, R.; Kasinathan, P.; Ramachandaramurthy, V.K.; Subramaniam, U.; Govindarajan, U.; Fernando, X. Intelligent optimization for charging scheduling of electric vehicle using exponential Harris Hawks technique. *Int. J. Intell. Syst.* **2021**, *36*, 5816–5844. [CrossRef]
5. Bremer, J.; Lehnhoff, S. Ant colony optimization for feasible scheduling of step-controlled smart grid generation. *Swarm Intell.* **2021**, *15*, 403–425. [CrossRef]
6. Yao, C.; Chen, S.; Yang, Z. Joint routing and charging problem of multiple electric vehicles: A fast optimization algorithm. *IEEE Trans. Intell. Transp. Syst.* **2021**, *23*, 8184–8193. [CrossRef]
7. Bi, X.; Chipperfield, A.J.; Tang, W.K.S. Coordinating electric vehicle flow distribution and charger allocation by joint optimization. *IEEE Trans. Ind. Inform.* **2021**, *17*, 8112–8121. [CrossRef]
8. Xiang, Y.; Yang, J.; Li, X.; Gu, C.; Zhang, S. Routing optimization of electric vehicles for charging with event-driven pricing strategy. *IEEE Trans. Autom. Sci. Eng.* **2021**, *19*, 7–20. [CrossRef]
9. Hu, D.; Huang, L.; Liu, C.; Liu, Z.W.; Ge, M.F. Data driven optimization for electric vehicle charging station locating and sizing with charging satisfaction consideration in urban areas. *IET Renew. Power Gener.* **2022**, *16*, 2630–2643. [CrossRef]
10. Niccolai, A.; Bettini, L.; Zich, R. Optimization of electric vehicles charging station deployment by means of evolutionary algorithms. *Int. J. Intell. Syst.* **2021**, *36*, 5359–5383. [CrossRef]
11. Rajamoorthy, R.; Arunachalam, G.; Kasinathan, P.; Devendiran, R.; Ahmadi, P.; Pandiyan, S.; Sharma, P. A novel intelligent transport system charging scheduling for electric vehicles using Grey Wolf Optimizer and Sail Fish Optimization algorithms. *Energy Sources Part A Recovery Util. Environ. Eff.* **2022**, *44*, 3555–3575. [CrossRef]
12. Król, A.; Sierpiński, G. Application of a genetic algorithm with a fuzzy objective function for optimized siting of electric vehicle charging devices in urban road networks. *IEEE Trans. Intell. Transp. Syst.* **2021**, *23*, 8680–8691. [CrossRef]
13. Cui, Y.; Hu, Z.; Duan, X. Optimal pricing of public electric vehicle charging stations considering operations of coupled transportation and power systems. *IEEE Trans. Smart Grid* **2021**, *12*, 3278–3288. [CrossRef]
14. Li, C.; Dong, Z.; Chen, G.; Zhou, B.; Zhang, J.; Yu, X. Data-driven planning of electric vehicle charging infrastructure: A case study of Sydney, Australia. *IEEE Trans. Smart Grid* **2021**, *12*, 3289–3304. [CrossRef]
15. Fakhrmoosavi, F.; Kavianipour, M.R.; Shojaei, M.H.; Zockaie, A.; Ghamami, M.; Wang, J.; Jackson, R. Electric vehicle charger placement optimization in michigan considering monthly traffic demand and battery performance variations. *Transp. Res. Rec.* **2021**, *2675*, 13–29. [CrossRef]
16. Zan, J. Research on robot path perception and optimization technology based on whale optimization algorithm. *J. Comput. Cogn. Eng.* **2022**, *1*, 201–208. [CrossRef]
17. Jia, Y.H.; Mei, Y.; Zhang, M. A bilevel ant colony optimization algorithm for capacitated electric vehicle routing problem. *IEEE Trans. Cybern.* **2021**, *52*, 10855–10868. [CrossRef]
18. Shi, L.; Zhan, Z.H.; Liang, D.; Zhang, J. Memory-based ant colony system approach for multi-source data associated dynamic electric vehicle dispatch optimization. *IEEE Trans. Intell. Transp. Syst.* **2022**, *23*, 17491–17505. [CrossRef]
19. Rostami, S.; Broumandnia, A.; Khademzadeh, A. An energy-efficient task scheduling method for heterogeneous cloud computing systems using capuchin search and inverted ant colony optimization algorithm. *J. Supercomput.* **2024**, *80*, 7812–7848. [CrossRef]
20. Gong, X.; Rong, Z.; Wang, J.; Zhang, K.; Yang, S. A hybrid algorithm based on state-adaptive slime mold model and fractional-order ant system for the travelling salesman problem. *Complex Intell. Syst.* **2023**, *9*, 3951–3970. [CrossRef]